

# SO(5) Invariance and Effective Field Theory for High $T_c$ Superconductors

C.P. Burgess<sup>a</sup> and C.A. Lütken<sup>b</sup>

<sup>a</sup> *Physics Department, McGill University*

*3600 University St., Montréal, Québec, Canada, H3A 2T8.*

<sup>b</sup> *Physics Department, University of Oslo*

*P.O. Box 1048, Blindern, N-0316 Norway.*

## Abstract

We set up the effective field theories which describe the  $SO(5)$ -invariant picture of the high- $T_c$  cuprates in various regimes. We use these to get *quantitative* conclusions concerning the size of  $SO(5)$ -breaking effects. We consider two applications in detail: (i) the thermodynamic free energy, which describe the phase diagram and critical behaviour, and (ii) the Lagrangian governing the interactions of the pseudo-Goldstone bosons with each other and with the electron quasiparticles deep within the ordered phases. We use these effective theories to obtain predictions for the critical behaviour near the possible bicritical point and the pseudo-Goldstone boson dispersion relations, as well as some preliminary results concerning their contribution to response functions. We systematically identify which predictions are independent of the microscopic details of the underlying electron dynamics, and which depend on more model-dependent assumptions.

## 1. Introduction and Summary

One of the remarkable features of high- $T_c$  cuprate materials is the basic connection they display between antiferromagnetism (AF) and superconductivity (SC). Indeed, any convincing theory of these materials must explain this fundamental property.

S.-C. Zhang [1] has recently argued for a new perspective on this AF-SC connection within the cuprates. He identifies an approximate  $SO(5)$  symmetry of the one-band Hubbard model which is believed to describe the dynamics of the pairing electrons within the  $Cu - O$  planes of these materials. This  $SO(5)$  symmetry contains as subgroups the  $SO(3)$  symmetry of spin rotations (which is spontaneously broken in the AF phase) and the electromagnetic  $SO(2)$  invariance (whose breaking defines the SC phase). From Zhang's vantage point both ordered phases arise once  $SO(5)$  is spontaneously broken, and the competition between antiferromagnetism and superconductivity becomes a 'vacuum alignment' problem, in which the direction of the order parameter is fixed by small effects which explicitly break the approximate  $SO(5)$  symmetry.

Evidence for the validity of this picture comes from the observation within the SC phase [2] of a collective mode, centred near momentum  $(\pi/a, \pi/a)$ , which couples to the spin-flip channel in neutron-scattering experiments. Its energy gap depends on doping in the same way as does  $T_c$  itself, taking the value  $\mathcal{E} \simeq 41$  meV at optimal doping. This state is understood in Zhang's framework as a pseudo-Goldstone boson (pGB) [3], whose gap is kept small compared to the underlying electron-electron interaction energy,  $J \simeq 0.1$  eV, by the  $SO(5)$  symmetry. Such a state is argued to be an approximate eigenstate of the Hubbard model Hamiltonian in refs. [4].

As is true for *any* physical system [5], the implications of the  $SO(5)$  picture at energies much lower than its intrinsic scale,  $J$ , may be efficiently encoded in terms of a low-energy effective theory. The effective theory which does so will depend on the symmetries and degrees of freedom which arise in the low-energy regime, and so can differ depending on the regimes of temperature or doping which are of interest.

Of particular interest are those low-energy predictions which depend only on the

symmetries and degrees of freedom of the low-energy theory, and not, say, on the values of the effective low-energy coupling constants. This is because such predictions are robust, in the sense that they are independent of the details of how these symmetries are realized by the underlying electron dynamics. This robustness obviously raises the stakes of the comparison with experiment, since disagreements cannot be attributed to small changes in microscopic details.

Our goal in the present paper is to pursue the ideas of ref. [1] by systematically exploring the low-energy effective theories which describe it in several regimes. A short summary of some of our results has been given in ref. [6]. We pause here to list some of our conclusions, before going into more detailed discussions in subsequent sections.

- (1) *The Phase Diagram:* Our first application is to the system's phase diagram. In §2, we consider the system's free energy, and use it to reiterate Zhang's description of the qualitative features of the phase diagram in the temperature-doping ( $T - x$ ) plane. We then extend this reasoning to argue that the *size* of the phases in this plane are related to the size of the  $SO(5)$ -breaking interactions, and so to the gaps for the pseudo-Goldstone states.

More precisely, suppose the system Hamiltonian (or Lagrangian) density has the form  $\mathcal{H} = \mathcal{H}_{\text{inv}} + \epsilon \mathcal{H}_{\text{sb}}$ , where  $\mathcal{H}_{\text{inv}}$  is  $SO(5)$  invariant, and  $\epsilon \ll 1$  quantifies the magnitude of the explicit  $SO(5)$ -breaking interactions at zero doping. We argue below that the gap for the pseudo-Goldstone state in the AF phase is  $\mathcal{E}_{AF} = O(\epsilon^{1/2}J)$ , while that in the SC phase is  $\mathcal{E}_{SC} = O(\epsilon^{1/3}J)$ . We learn the size of  $\epsilon$  from the observed 41 meV gap of the SC phase:  $\epsilon \sim 0.01$ . Both the Néel temperature at zero doping ( $T_N$ ), and the SC critical temperature at optimal doping ( $T_c$ ), are predicted to be of order  $\epsilon^{1/2}J$ , leading to the (correct) expectation that these should be of order  $100K$ .

Similar statements hold for the doping required at zero temperature to destroy the AF order and enter the SC regime. This transition is predicted for dopings of order  $x_c \simeq \epsilon^{1/2} \simeq 10\%$ . In addition, a potential 'mixed' phase (MX), which is both AF and SC in nature, can arise between the purely SC and AF phases, again over a range of dopings which is of order  $\epsilon^{1/2} \simeq 10\%$ . The superconducting phase itself is expected to extend out

to dopings for which the  $SO(5)$  invariance is no longer a good approximation.

Although the  $O(1)$  prefactors to these estimates are model dependent, and so will vary from material to material, the general shape of the resulting phase diagram should be shared by all high- $T_c$  systems, and seems to agree reasonably well with the typical experimental phase diagram [7].

- (2) *Critical Behaviour*: The high- $T_c$  systems differ from traditional superconductors in that they display critical behaviour within a few degrees of  $T_c$ . This critical behaviour is the topic of §2.3. The  $SO(5)$ -invariant scheme predicts the usual scaling behaviour for the transitions from the SC or AF regimes into the disordered phase. It makes different predictions for the vicinity of a potential bicritical (or tetracritical) point which is expected should the SC and AF phases coexist for some temperatures and dopings. Zhang has argued that one is attracted here to an  $SO(5)$ -invariant fixed point, based on the  $d = 2 + \varepsilon$  expansion for  $d$ -dimensional nonlinear sigma-models. We point out here an alternative possibility where the stable fixed point weakly breaks  $SO(5)$ , based on the  $d = 4 - \varepsilon$  expansion, and compute the critical exponents in this picture.

- (3) *Pseudo-Goldstone Boson Spectrum*: Next, §3 applies  $SO(5)$  to the underlying Hamiltonian for energies, temperatures and dopings corresponding to the ordered phases, and obtains the properties of the pseudo-Goldstone modes. As was emphasized elsewhere [6], since there are more features to these gap spectra than there are parameters in the general effective theory, it is possible to predict low-energy relations amongst the various features of the dispersion relations for these states.

Model-independent, weak-coupling conclusions do not appear to be possible for the disordered phase, although inferences regarding this phase may be made by making more specific use of additional assumptions concerning the microscopic dynamics.

Our pGB Lagrangian differs in detail from that proposed by Zhang, since it involves a few more terms. Although they completely agree for qualitative purposes, we argue the inclusion of the most general interactions is required to permit the robust inference of the quantitative size of symmetry-breaking effects.

- (4) *Response Functions*: Finally, §4 uses the effective theory to make some preliminary points concerning the pseudo-Goldstone boson contributions to electromagnetic and spin response functions within the AF and SC phases. In particular, the origin within the effective theory, of the pseudo-Goldstone pole in the SC-phase spin response is identified.

## 2. Implications for Thermodynamics

In terms of the underlying electrons, the ordered AF and SC phases of the high- $T_c$  systems are distinguished by nonzero values for the order parameters  $\langle \psi_p(i\sigma^2)\psi_{-p} \rangle$  and  $\langle \psi_{p+Q}^\dagger \sigma^a \psi_p \rangle$ , where  $p$  is an electron momentum,  $Q = (\frac{\pi}{a}, \frac{\pi}{a})$  and  $\sigma^a$  denotes the Pauli matrices. Long-wavelength variations of these quantities can therefore be described by the fields:

$$n_Q(k) \propto \psi_{p+k}(i\sigma_2)\psi_{-p} \quad \text{and} \quad n_S^a(k) \propto \psi_{p+Q+k}^\dagger \sigma^a \psi_p, \quad (1)$$

where  $k$  is much smaller than either  $p$  or  $Q$ .

In Zhang's framework, in addition to the  $SO(3) \times SO(2)$  symmetry of spin and electromagnetic gauge transformations there are approximate symmetries which rotate  $n_Q$  and  $n_S$ , into one another. To represent this symmetry it is convenient to group  $n_Q$  and  $n_S$  into a real, five-dimensional quantity

$$\mathbf{n} = \begin{pmatrix} n_Q \\ n_S \end{pmatrix}, \quad (2)$$

on which the extended symmetry acts by matrix multiplication on the left by an orthogonal five-by-five matrix:  $\mathbf{n} \rightarrow O \mathbf{n}$ , where  $O$  is an arbitrary five-by-five orthogonal matrix. This identifies the electromagnetic  $SO(2)$  and spin  $SO(3)$  subgroups as the block-diagonal combinations:

$$O = \begin{pmatrix} SO(2) & 0 \\ 0 & SO(3) \end{pmatrix}. \quad (3)$$

We denote by  $T_\alpha$  the hermitian, antisymmetric five-by-five matrices which generate  $SO(5)$ , with the special cases of the generators of  $SO(2)$  and  $SO(3)$  represented by:

$$Q = q \begin{pmatrix} \sigma^2 & \\ & 0 \end{pmatrix}, \quad \text{and} \quad \vec{T} = \begin{pmatrix} 0 & \\ & \vec{t} \end{pmatrix}. \quad (4)$$

Here  $q = 2$  is the electric charge of the order parameter in units of the electron charge and  $\vec{t}$  are a basis of three-by-three generators of  $SO(3)$ .

The resulting  $SO(5)$  symmetry is simultaneously subject to two kinds of breaking. On one hand it is broken explicitly (but weakly) to the exact  $SO(3) \times SO(2)$  subgroup by the electron Hamiltonian, and on the other hand it is spontaneously broken to  $SO(4)$ . What follows in this section spells out our assumptions concerning how this symmetry manifests itself in thermodynamic functions.

## 2.1) Thermodynamic Potentials

Given this picture we may write the free-energy density,  $f$ , as the sum of an  $SO(5)$ -invariant term,  $f_{\text{inv}}$ , and a small  $SO(5)$ -breaking term,  $f_{\text{sb}}$ . For a slowly varying order parameter we may use a derivative expansion of  $f$ , leading to the following most general expressions for time-independent  $n_Q$  and  $n_S$ :<sup>1</sup>

$$\begin{aligned}
\beta f_{\text{inv}} &= v_{\text{inv}} + w_{\parallel}^{(+)} \left( \nabla_a n_Q \cdot \nabla_a n_Q + \nabla_a n_S \cdot \nabla_a n_S \right) + u_{\parallel}^{(+)} \left( n_Q \cdot \nabla_a n_Q + n_S \cdot \nabla_a n_S \right)^2 \\
&\quad + w_{\perp}^{(+)} \left( \nabla_c n_Q \cdot \nabla_c n_Q + \nabla_c n_S \cdot \nabla_c n_S \right) + u_{\perp}^{(+)} \left( n_Q \cdot \nabla_c n_Q + n_S \cdot \nabla_c n_S \right)^2 + \dots, \\
\beta f_{\text{sb}} &= v_{\text{sb}} + w_{\parallel}^{(-)} \left( \nabla_a n_Q \cdot \nabla_a n_Q - \nabla_a n_S \cdot \nabla_a n_S \right) + u_{\parallel}^{(-)} \left( n_Q \cdot \nabla_a n_Q - n_S \cdot \nabla_a n_S \right)^2 \\
&\quad + w_{\perp}^{(-)} \left( \nabla_c n_Q \cdot \nabla_c n_Q - \nabla_c n_S \cdot \nabla_c n_S \right) + u_{\perp}^{(-)} \left( n_Q \cdot \nabla_c n_Q - n_S \cdot \nabla_c n_S \right)^2 \\
&\quad + u_{\parallel}^{(0)} n_Q \cdot \nabla_a n_Q n_S \cdot \nabla_a n_S + u_{\perp}^{(0)} n_Q \cdot \nabla_c n_Q n_S \cdot \nabla_c n_S + \dots.
\end{aligned} \tag{5}$$

Here  $\beta = 1/kT$ , and the ellipses represent terms involving more derivatives than two. The coefficient functions,  $v_{\text{inv}}, v_{\text{sb}}, w_{\perp}^{(\pm)}, w_{\parallel}^{(\pm)}, u_{\perp}^{(\pm,0)}$  and  $u_{\parallel}^{(\pm,0)}$  are potentially arbitrary functions of the  $SO(3) \times SO(2)$  invariants  $n_Q \cdot n_Q$  and  $n_S \cdot n_S$ . They depend as well on the two thermodynamic variables: temperature and doping (more about this dependence below). Keeping in mind the anisotropy of the cuprate systems, separate coefficients are

---

<sup>1</sup> This expression differs from that of refs. [1], [8] in three ways. Besides working in the isotropic limit, these authors: (1) impose the constraint  $n_S \cdot n_S + n_Q \cdot n_Q = 1$ , (2) keep only three of the lowest terms in an expansion of the  $w$ 's and  $u$ 's in powers of fields, and (3) keep only quadratic terms in the potential  $v$ . (Their quartic interactions arise from the chemical-potential dependence of the terms involving two derivatives of  $n_Q$ .) We comment further on these differences as they arise at subsequent points in the text.

included for derivatives,  $a = x, y$ , parallel to the copper oxide planes, and those,  $c = z$ , perpendicular to this plane. For simplicity we assume rotational symmetry within the planes.

In the limit of  $SO(5)$  invariance,  $v_{\text{sb}} = w_{\perp}^{(-)} = w_{\parallel}^{(-)} = u_{\perp}^{(-)} = u_{\parallel}^{(-)} = u_{\perp}^{(0)} = u_{\parallel}^{(0)} = 0$ , and each of the remaining functions  $v_{\text{inv}}, w_{\perp}^{(+)}, w_{\parallel}^{(+)}, u_{\perp}^{(+)}$  and  $u_{\parallel}^{(+)}$  depend only on the combination  $\mathbf{n} \cdot \mathbf{n} = n_Q \cdot n_Q + n_S \cdot n_S$ .

The predictive power of the approximate symmetry comes from computing observables perturbatively in the small symmetry-breaking interactions. Doing so requires a quantitative characterization of the size of the symmetry-breaking terms in  $f$ . We imagine, therefore, the microscopic electronic Hamiltonian to have the generic form:

$$\mathcal{H} = \mathcal{H}_{\text{inv}} + \epsilon \mathcal{H}_{\text{sb}} - \mu \mathcal{Q}, \quad (6)$$

where  $\mathcal{H}_{\text{inv}}$  preserves  $SO(5)$ , while  $\mathcal{H}_{\text{sb}}$  and  $\mu \mathcal{Q}$  both break it.  $\mu$  here is the chemical potential for the electric charge,  $\mathcal{Q}$ . We take  $\mu = 0$  to correspond to half filling.

Notice that  $SO(5)$  symmetry is explicitly broken in two different ways in eq. (6), and so there are two different parameters,  $\epsilon$  and  $\mu$ , which govern the symmetry-breaking terms in the free energy,  $f$ :

- *Zero Doping:* Things are simplest at half filling, for which  $\mu = 0$  and so only one  $SO(5)$ -breaking parameter exists:  $\epsilon$ . Based on our later discussion of the spectrum of the gap in the pseudoGoldstone boson spectrum in the SC phase, we take in what follows  $\epsilon \simeq 0.01$ . It is this small parameter which ultimately determines the size of the different phases in the system's phase diagram.

- *Nonzero Doping:* The second source of explicit  $SO(5)$  breaking in eq. (6) is the chemical potential,  $\mu$ , which is introduced to describe the doping of high- $T_c$  systems away from half filling. This breaks  $SO(5)$  because  $\mu$  couples only to electric charge, which is just one of the ten  $SO(5)$  generators. For thermodynamic applications it is more convenient to trace the dependence of the free energy on the number density of charge carriers,  $n$ , rather than  $\mu$ , and so we define the doping,  $x$ , by  $n = x/\mathcal{V}$ , with  $\mathcal{V}$  the volume of a unit cell. In typical

high- $T_c$  systems at zero temperature,  $x \lesssim 10\%$  is characteristic of the AF phase, while  $0.1 \lesssim x \lesssim 0.4$  is representative of the SC phase [7].

To explore the implications of these two sources of symmetry breaking we consider first the classical phase transitions which are implied by the choice of an  $SO(5)$  invariant order parameter.

## 2.2) Classical Phase Transitions

For a classical phase transition the free energy density,  $f(x, T, n_Q, n_S)$ , is assumed to admit a Taylor expansion in powers of  $n_Q$  and  $n_S$  near  $n_Q = n_S = 0$ . This assumption of analyticity at zero field is known to fail in the vicinity of a critical point, where the long-distance fluctuations can cause  $f$  to acquire a singular dependence on its arguments. For temperatures closer to  $T_c$  than a few degrees, the resulting critical behaviour is poorly described by a classical discussion. Unlike traditional superconductors, the correlation length in high- $T_c$  systems is sufficiently small to permit critical behaviour to be observed, although typically only within a few degrees of  $T_c$  [9].

For these reasons we expect a classical analysis to be adequate for the purposes of identifying the overall size occupied by the various phases within the phase diagram in the  $T - x$  plane. We investigate the implications of  $SO(5)$  for the critical behaviour in §2.3, below.

We start by rederiving Zhang's treatment of classical phase transitions. Our addition to his argument is the quantifying of the size of the symmetry-breaking effects in this analysis. Consider therefore expanding the potential  $v$  to quartic order in the order parameters,  $n_Q$  and  $n_S$ :<sup>2</sup>

$$v = v_{00} + \frac{1}{2} \left( v_{20} n_Q \cdot n_Q + v_{02} n_S \cdot n_S \right) + \frac{1}{4} \left[ v_{40} (n_Q \cdot n_Q)^2 + v_{22} n_Q \cdot n_Q n_S \cdot n_S + v_{04} (n_S \cdot n_S)^2 \right] + \dots, \quad (7)$$

---

<sup>2</sup> This potential corrects a minor error [10] in the potential in the original version of ref. [6], although none of the results of this reference are altered by this change.



where the coefficients,  $v_{jk}$ , are regarded as functions of the thermodynamic variables,  $x$  and  $T$ , as well as the small symmetry-breaking parameter  $\epsilon$ . Particle-hole symmetry<sup>3</sup> further implies  $v_{jk}$  must also satisfy  $v_{jk}(-x) = v_{jk}(x)$ , if  $T$  and  $\epsilon$  are held fixed.

Next divide this expression into its  $SO(5)$ -invariant and -breaking parts,  $v = v_{\text{inv}} + v_{\text{sb}}$ , where:

$$\begin{aligned} v_{\text{inv}} &= v_{00} + \frac{\rho}{2} (n_Q \cdot n_Q + n_S \cdot n_S) + \frac{\lambda}{4} (n_Q \cdot n_Q + n_S \cdot n_S)^2 + \dots, \\ v_{\text{sb}} &= \frac{g}{2} (n_Q \cdot n_Q - n_S \cdot n_S) + \frac{k}{4} (n_Q \cdot n_Q - n_S \cdot n_S)^2 + \frac{h}{4} [(n_Q \cdot n_Q)^2 - (n_S \cdot n_S)^2] + \dots \end{aligned} \quad (8)$$

The parameters in these expressions are related as follows:  $v_{02} = \rho - g$ ,  $v_{20} = \rho + g$ ,  $v_{40} = \lambda + k + h$ ,  $v_{04} = \lambda + k - h$  and  $v_{22} = \lambda - k$ .

Phase	Minimum	Conditions
Normal (N)	$ n_Q  =  n_S  = 0$	$v_{20} > 0, v_{02} > 0$
Superconductor (SC)	$ n_Q  \neq 0,  n_S  = 0$	$v_{20} < 0, v_{02} > 0$
Antiferromagnet (AF)	$ n_Q  = 0,  n_S  \neq 0$	$v_{20} > 0, v_{02} < 0$
Mixed (MX)	$ n_S  \neq 0,  n_Q  \neq 0$	$v_{20} < 0, v_{02} < 0, k > 0$

**Table I**

The possible minima of the free energy density,  $v$ , each distinguished by the sign of  $v_{02}$  and  $v_{20}$ . Two possibilities arise if both of these parameters are negative, depending on the sign taken by the quartic coupling,  $k$ .  $k > 0$ , defines a minimum for which both  $|n_S|$  and  $|n_Q|$  are nonzero. If  $k < 0$ , then there is both AF and SC type minima, separated by an energy barrier. The corresponding phase diagram in the  $\rho$ - $g$  plane is given for both choices for  $k$  in Fig. (1).

Minimization of this potential gives four kinds of phases depending on whether  $n_S$  and/or  $n_Q$  vanish at the minimum. These four alternatives are controlled, in first approximation, by the signs of the coefficients of the two quadratic terms,  $v_{20}$  and  $v_{02}$ , as outlined in Table I. The case where both  $v_{20}$  and  $v_{02}$  are negative, further subdivides into two

<sup>3</sup> Alternatively, the same conclusion is also drawn in later sections by considering the free energy to be a function of  $\mu$  rather than  $x$ , and using the antisymmetry of  $Q$ . See also [6].

alternatives which are distinguished by the sign of the quartic coupling,  $k$ . If  $k > 0$  then both  $|n_Q|$  and  $|n_S|$  are nonzero at the minimum, while if  $k < 0$  then two types of minima coexist, which differ according to whether it is  $|n_S|$  or  $|n_Q|$  which is nonzero. When  $k < 0$  these two minima are separated by an energy barrier.

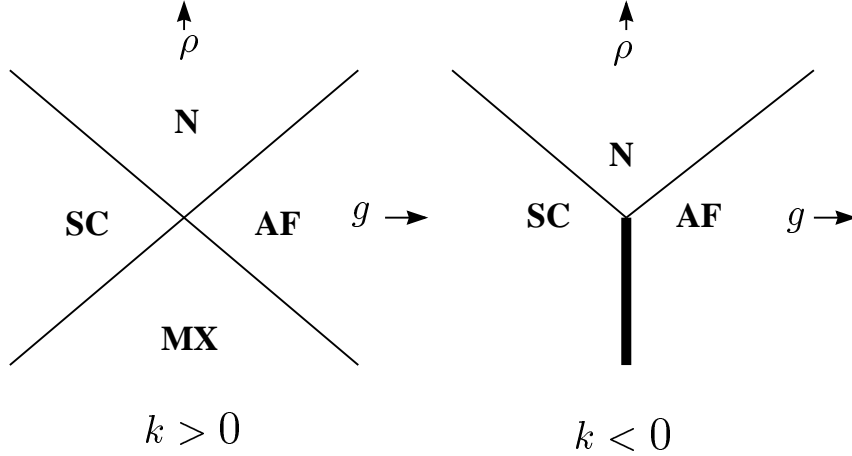


**Figure 1**

The phase diagram for the free energy function described in the text in the  $\rho - g$  plane, where  $\rho$  is the  $SO(5)$ -symmetric, and  $g$  is the  $SO(5)$ -breaking, quadratic couplings in the free energy. The thin lines represent second-order transition lines, while the fat line is a first-order phase boundary. The two possibilities portrayed are distinguished by the sign of the quartic coupling,  $k$ , in the free energy.

The corresponding phase diagram, in the  $\rho - g$  plane, is drawn in Fig. (1). When  $k > 0$  there are four phases, and all phase boundaries define second-order transitions. The four phase boundaries intersect at a tetracritical point, which is defined by  $\rho = g = 0$ . When  $k < 0$  there are only three phases, with the antiferromagnetic (AF) and superconducting (SC) regions meeting at a first-order transition. This phase boundary intersects the second-order boundaries with the disordered phase (N) at a bicritical point, again at  $\rho = g = 0$ . The picture which emerges is the semiclassical phase diagram described in ref. [1].

More information becomes available, however, once the dependence of the transition

regions on the small symmetry-breaking quantity  $\epsilon \simeq 0.01$  is included. To see this, imagine examining  $v$  in the vicinity of half filling, where  $x \ll 1$ . Keeping in mind that all  $SO(5)$ -breaking interactions must vanish if both  $x$  and  $\epsilon$  do, and that  $v_{jk}$  must be even functions of  $x$ , we write in this limit:

$$g = \epsilon g_0 + g_2 x^2 + g_4 x^4 + \dots, \quad h = \epsilon h_0 + h_2 x^2 + h_4 x^4 + \dots, \quad k = \epsilon k_0 + k_2 x^2 + k_4 x^4 + \dots, \quad (9)$$

where the coefficients of this expansion are functions of  $T$  which can be unsuppressed by additional powers of  $\epsilon$  or  $x$ .

Since the  $SO(5)$ -invariant couplings need not vanish with either  $\epsilon$  or  $x$ , for them we instead write:

$$\lambda = \lambda_0 + \lambda_2 x^2 + \lambda_4 x^4 + \dots \quad (10)$$

The  $SO(5)$ -invariant quadratic term must be handled more carefully, however. This is because real high- $T_c$  systems are antiferromagnets at zero temperature and doping, and so we have the important additional information  $v_{20}(T = x = 0) > 0$  and  $v_{02}(T = x = 0) < 0$ . Equivalently this implies:  $g(T = x = 0) > 0$  and  $-g(T = x = 0) < \rho(T = x = 0) < g(T = x = 0)$ , which is only consistent with  $g(T = x = 0) = O(\epsilon)$  if  $\rho(T = x = 0)$  is also  $O(\epsilon)$ . We take, therefore, at zero temperature:

$$\rho = \epsilon \rho_0 + \rho_2 x^2 + \rho_4 x^4 + \dots \quad (11)$$

- *Transition Dopings:*

These expansions determine the domains of doping over which the various phases are possible, so long as  $x$  is small. For temperatures below the Néel temperature – and so for which  $-g_0 < \rho_0 < g_0$  – define  $x_{AF}$  as the doping above which the AF order is lost.  $x_{AF}$  is then determined by the requirement that  $v_{02} = \rho - g = 0$ , for which eqs. (10) and (11) imply:

$$x_{AF}^2 = -\epsilon \left( \frac{\rho_0 - g_0}{\rho_2 - g_2} \right) + O(\epsilon^2). \quad (12)$$

So long as both numerator and denominator are both order unity, and  $\rho_2 > g_2$ , we see the prediction is:  $x_{AF} = O(\epsilon^{1/2}) \simeq 10\%$ , which agrees well with what is observed for real high- $T_c$  systems.

Similarly, a superconducting phase arises for dopings greater than  $x_{SC}$ , defined as the value of  $x$  for which  $v_{20} = \rho + g = 0$ . Again eqs. (10) and (11) give:

$$x_{SC}^2 = -\epsilon \left( \frac{\rho_0 + g_0}{\rho_2 + g_2} \right) + O(\epsilon^2), \quad (13)$$

and so  $x_{SC}$  is also predicted to be  $O(\epsilon^{1/2}) \simeq 10\%$ , so long as numerator and denominator are  $O(1)$  and  $\rho_2 + g_2 < 0$ .

If we instead work to  $O(x^4)$  in  $v_{20}$ , then a second root  $x'_{SC}$  can develop beyond which superconductivity is again lost. As is easy to see, this second root arises for  $x \simeq O(1)$ , and so lies outside of the domain of the small- $x$  expansion, and for  $x$  potentially large enough to invalidate the approximate  $SO(5)$  symmetry. Notice that this implies that the optimal doping,  $x_{opt}$  — defined as the doping for which  $T_c$  is largest — is also  $O(1)$ , and so is unsuppressed by powers of  $\epsilon$ .

Finally, if  $x_{AF} > x_{SC}$ , and if  $k > 0$ , then dopings satisfying  $x_{SC} < x < x_{AF}$  give both a superconductor and an antiferromagnet (as in the MX phase) at zero temperature. This phase can extend over a range of dopings which is at most as large as  $x_{AF} - x_{SC} = O(\epsilon^{1/2})$ . Otherwise, if  $k < 0$ , the AF to SC transition is first order.

- *Transition Temperatures:* Similar arguments may be applied to estimate the size of the critical temperatures for the various ordered phases if the  $T$  dependence of the coefficients in  $v$  is known. In mean-field theory the large-temperature limit of the temperature dependence of the free energy may be argued on dimensional grounds. For large  $T$  in  $d$  dimensions, the quadratic coefficients,  $\rho$  and  $g$ , are proportional to  $T^2$ , with a prefactor that can be  $O(1)$  for  $\rho$ , but which is suppressed by  $\epsilon$  or  $x^2$  for  $g$ .

For sufficiently large  $T$  it follows that eventually  $\rho > |g|$ , implying a transition to the disordered phase (N). The transition temperature as a function of doping may be estimated by asking when the  $T^2$  contribution is the same size as is the zero-temperature values of

for  $\rho$  and  $g$ . Since the zero-temperature limits of both  $\rho$  and  $g$  are suppressed by powers of  $\epsilon$  and/or  $x^2$ , the transition temperature,  $T_c$ , is predicted to be smaller than might be expected based on the underlying electronic scales,  $J \simeq 0.1 \text{ eV} \simeq 1000 \text{ K}$ . At zero doping only  $\epsilon$  controls the size of symmetry breaking, so the Néel temperature,  $T_N$ , is expected to be

$$T_N = O(\epsilon^{1/2}J) \simeq 100 \text{ K}. \quad (14)$$

Once again this is the right order of magnitude for the cuprates. Of course, these estimates can be further reduced by other effects. For example, very anisotropic systems are effectively two dimensional, in which case  $w_{\perp}^{(\pm)}, u_{\perp}^{(\pm,0)} \rightarrow 0$ , implying  $T_c \rightarrow 0$ .

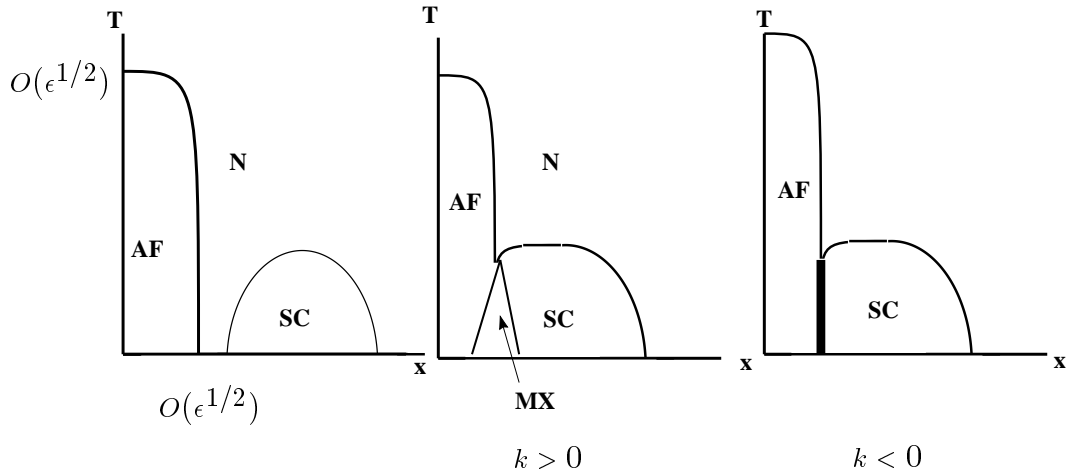


**Figure 2**

The phase diagram for the free energy function described in the text in the temperature–doping plane. As for Fig. (1), the thin lines represent second-order transition lines, while the fat line is a first-order phase boundary. The two possibilities for which the AF and SC phases coexist are distinguished by the sign of the quartic coupling,  $k$ , in the free energy.

We are thus led to the phase diagram of Fig. (2) in the temperature–doping plane, which reproduces well the generic features of the phase diagram for real high- $T_c$  systems.

### 2.3) Critical Behaviour

Since the symmetry of the order parameter has important implications for the critical exponents, and since some critical behaviour is experimentally accessible for the cuprates, we pause to explore critical phenomena more carefully here.

As is well known, in  $d < 4$  dimensions the Gaussian fixed point is unstable in the infrared, and so the critical exponents are controlled by some other infrared fixed point of the renormalization group. In the absence of more reliable methods, one is reduced to expanding about either the upper ( $d = 4$ ) or lower ( $d = 2$ ) critical dimensions. Our approach here is to expand in powers of  $d - 4$ , and we do so for both the critical lines separating the disordered (N) phase from the others, as well as for the bi- or tetra-critical point should these lines meet. We imagine in what follows that all five of the fields in  $n_S$  and  $n_Q$  are free to fluctuate. Our treatment of the tetracritical point therefore differs from Zhang's, since he draws his conclusions for this point using the nonlinear sigma model, for which  $n_S \cdot n_S + n_Q \cdot n_Q = 1$ , based on an expansion about  $d = 2$  [11].

Along the critical line the  $SO(5)$  picture implies the usual  $O(N)$ -invariant infrared fixed points, where  $N = 3$  for the Néel transition, and  $N = 2$  (XY universality [12]) for the superconducting transition<sup>4</sup>. Both are covered by the usual result to leading order in the expansion in  $\varepsilon = 4 - d$ :

$$\frac{v_*}{8\pi^2} = \frac{\varepsilon}{N + 8} + O(\varepsilon^2), \quad \frac{1}{\nu} = 2 - \frac{N + 2}{N + 8} \varepsilon + O(\varepsilon^2), \quad (15)$$

where  $v_*$  denotes the fixed-point value of  $v_{40}$  for the N/SC transition (or of  $v_{04}$  for the N/AF transition).<sup>5</sup>  $\nu$  is the standard critical exponent for the correlation length, which diverges like  $\xi \sim t^{-\nu}$  as  $t \equiv T/T_c - 1 \rightarrow 0$ . There is indeed good experimental evidence [9] that  $\nu$  for the N/SC transition, is given as predicted for XY universality.

The fixed point behaviour in the bicritical (or tetracritical) region differs qualitatively from that found along the two critical lines. This is because the  $O(N)$ -invariant fixed

---

<sup>4</sup> Due to the relevance of the electromagnetic coupling, the SC transition crosses over from XY universality to that of a charged fluid, although undetectably close to  $T_c$  [12].

<sup>5</sup> Very near the critical point (and so in this section only) we ignore the system's anisotropy and rescale all fields to canonically normalize the derivative terms in the free energy.

point is stable only for  $N < 4 - O(\varepsilon)$ , and so does not apply for  $N = 5$ . The fixed point appropriate for  $N = 5$  may be found numerically, and the results obtained agree where they can be compared with previous treatments [13], as well as with the approximate analytic expressions given below.

In order to identify the fixed points it is useful to consider a model for which the field  $n_s$  spans an  $N_s$ -dimensional space, and  $n_Q$  spans a space of  $N_Q$  dimensions. The free energy is assumed to be  $O(N_s) \times O(N_Q)$  invariant. In this case useful approximate expressions for the fixed points may be derived in an expansion in powers of  $n \equiv N_s - N_Q$  over  $\bar{N} = N_s + N_Q$ . In the case of present interest  $N_s = 3$  and  $N_Q = 2$ , and so the parameter  $n/\bar{N} = 1/5$  is reasonably small.

The stable fixed points which emerge at leading order in  $\varepsilon = 4 - d$  then are: (i) the  $O(\bar{N})$ -invariant fixed point, for  $\bar{N} < 4$ ; (ii) the ‘decoupled’ fixed point (for which  $(v_{22})_* = 0$ ), for  $(N_s + 2)(N_Q + 2) > 36$ ; and (iii) a third fixed point for intermediate values of  $N_s$  and  $N_Q$ . It is this third fixed point which is appropriate for  $N_s = 3$  and  $N_Q = 2$ , and it gives:

$$\frac{\lambda_*}{4\pi^2} \approx 8 \lambda_0, \quad \frac{h_*}{4\pi^2} \approx \frac{n(\bar{N} - 4)}{\bar{N} - 2} \lambda_0, \quad \frac{k_*}{4\pi^2} \approx 2(\bar{N} - 4) \lambda_0, \quad (16)$$

where  $\lambda_0 \equiv \varepsilon/(\bar{N}^2 + 32)$ . For  $\bar{N} = 5$ ,  $n = 1$  and  $d = 3$  these expressions agree well with the values we obtained numerically to linear order in  $\varepsilon$ :  $\lambda_*/(4\pi^2) \approx 0.141$ ,  $h_*/(4\pi^2) \approx 0.00573$ , and  $k_*/(4\pi^2) \approx 0.0340$ . Notice the hierarchy  $h_* \ll k_* \ll \lambda_*$  which is satisfied at this fixed point, and is consistent with approximate  $SO(5)$  invariance, albeit with some symmetry-breaking couplings which are larger than  $O(1\%)$  of their  $SO(5)$ -invariant counterparts.

Since the picture of how the critical lines merge near the bicritical point differs somewhat from that of ref. [1], we next present this in more detail. The running of the two

quadratic couplings,  $\rho$  and  $g$ , in the far infrared is given near the fixed point by:

$$\begin{aligned}
\left(\mu \frac{\partial \rho}{\partial \mu}\right)_* &= -2\rho + \frac{1}{16\pi^2} \left\{ \left[ 2(\bar{N} + 2)\lambda_* + 4k_* - nh_* \right] \rho + \left[ (\bar{N} + 4)h_* - 2n\lambda_* \right] g \right\}, \\
&= -2\rho + \frac{\lambda_0}{4(\bar{N} - 2)} \left\{ \left[ 24\bar{N}(\bar{N} - 2) - n^2(\bar{N} - 4) \right] \rho + \left[ (\bar{N} - 8)^2 - 48 \right] n g \right\}, \\
\left(\mu \frac{\partial g}{\partial \mu}\right)_* &= -2g + \frac{1}{16\pi^2} \left\{ \left[ (\bar{N} + 4)h_* - 2nk_* \right] \rho + \left[ 4\lambda_* + 2(\bar{N} + 2)k_* - nh_* \right] g \right\}, \\
&= -2g + \frac{\lambda_0}{4(\bar{N} - 2)} \left\{ -3n(\bar{N} - 4)^2 \rho + \left[ 4\bar{N}(\bar{N} - 2)^2 - n^2(\bar{N} - 4) \right] g \right\}.
\end{aligned} \tag{17}$$

The principal directions of the flow, and the corresponding scaling exponents, near the fixed point are given to good approximation by:

$$\rho_+ \approx \rho - \left( \frac{3n(\bar{N} - 4)^2}{4\bar{N}(\bar{N} - 2)(8 - \bar{N})} \right) g \quad \rho_- \approx g - \left( \frac{n[(\bar{N} - 8)^2 - 48]}{4\bar{N}(\bar{N} - 2)(8 - \bar{N})} \right) \rho \tag{18}$$

and:

$$\frac{1}{\nu_+} \approx 2 - \frac{6\bar{N}}{\bar{N}^2 + 32} \varepsilon, \quad \frac{1}{\nu_-} \approx 2 - \frac{\bar{N}(\bar{N} - 2)}{\bar{N}^2 + 32} \varepsilon. \tag{19}$$

For  $\bar{N} = 5$  and  $n = 1$  these become  $\rho_+ \simeq \rho - 0.017 g$  and  $\rho_- \simeq g + 0.22 \rho$ , while  $\nu_+ \simeq 0.68$  and  $\nu_- \simeq 0.58$ .

The largest of these exponents defines the temperature exponent,  $\nu = \nu_+ \simeq 0.68$ . The scaling form for the free energy density,  $f = t^{-d\nu} \mathcal{F} \left( \frac{\rho_-}{t^\phi} \right)$ , defines the crossover exponent,  $\phi$ , which is given by  $\phi = \nu_+ / \nu_-$ . We have:

$$\phi \approx \frac{\bar{N}^2 + 2\bar{N} + 64}{2(\bar{N}^2 - 3\bar{N} + 32)} \simeq 1.2. \tag{20}$$

Since  $\phi > 1$ , the two critical lines approach the bicritical point tangent to one another, and to the line  $\rho_- = 0$  — or, equivalently, to the line  $g = \left( \frac{n[(\bar{N} - 8)^2 - 48]}{4\bar{N}(\bar{N} - 2)(8 - \bar{N})} \right) \rho \simeq 0.22 \rho$ .

It would obviously be of great interest to examine experimentally the critical behaviour at the bicritical point, since this would more decisively distinguish the symmetries of the order parameter at this point. Unfortunately, to our knowledge, there is currently no



experimental information concerning this critical behaviour, likely due to the disorder which is introduced in this region by the doping process.

### 3. The Nonlinear Sigma Model: Pseudo-Goldstone Modes

More microscopically, another regime for which  $SO(5)$ -invariance provides definite quantitative predictions is deep within the ordered phases. Here the low-energy dynamics is governed by the Goldstone, and pseudo-Goldstone modes, together with their interactions with the other low-energy degrees of freedom. Much can be said about these low-energy properties because low-energy Goldstone-boson dynamics is largely determined purely by the pattern of spontaneous symmetry breaking [5], [14], [15].

The present section is devoted to developing the quantitative description of this regime. Section §3.1 first describes the most general low-energy effective Lagrangian for this phase, which is then used in §3.2 to determine the dispersion relations for the pseudo-Goldstone bosons themselves. Their interactions are used in §4 to draw preliminary conclusions about their contributions to response functions in the AF and SC phases, which also involves their interactions with the low-energy electron-like quasiparticles.

#### 3.1) *The Effective Lagrangian*

Imagine, then, that  $T$  and  $x$  are chosen to lie within one of the ordered phases, and integrating out all degrees of freedom which involve energies larger than some scale,  $\Lambda$ . We wish to write down the effective Lagrangian governing the degrees of freedom which remain at still lower energies. Although this effective Lagrangian cannot yet be derived from the microscopic physics, we are guaranteed to capture its physics so long as we use the *most general possible* Lagrangian involving the low-energy modes and respecting all of the symmetries [5].

When a global symmetry,  $G$ , is spontaneously broken to a subgroup,  $H$ , the self-couplings and spectrum of the resulting (pseudo-) Goldstone states is described at low energies by the nonlinear sigma model for the quotient space  $G/H$  [5], [14], [15]. When

$G = SO(5)$  and  $H = SO(4)$  this implies the lowest terms in the derivative expansion of the Lagrangian for this system are completely determined by two constants. Of course, more possibilities arise once explicit  $SO(5)$ -breaking interactions are introduced.

The most general such Lagrangian involving two or fewer derivatives is again built from the fields  $n_S$  and  $n_Q$ , but with the important difference, relative to §2.1, that these now satisfy the constraint  $n_S \cdot n_S + n_Q \cdot n_Q \equiv 1$ , since we are interested in only the Goldstone and pseudo-Goldstone modes. In the absence of doping, the result takes a form which is similar to eq. (5),  $\mathcal{L} = \mathcal{L}_{\text{inv}} + \mathcal{L}_{\text{sb}}$ , with: <sup>6</sup>

$$\begin{aligned} \mathcal{L}_{\text{inv}} &= \frac{f_t^2}{2} \left( \partial_t n_Q \cdot \partial_t n_Q + \partial_t n_S \cdot \partial_t n_S \right) - \frac{f_{\parallel}^2}{2} \left( \nabla_a n_Q \cdot \nabla_a n_Q + \nabla_a n_S \cdot \nabla_a n_S \right) \\ &\quad + \frac{f_{\perp}^2}{2} \left( \nabla_c n_Q \cdot \nabla_c n_Q + \nabla_c n_S \cdot \nabla_c n_S \right) + \dots \\ \mathcal{L}_{\text{sb}} &= -V + f_t^2 \left[ A \partial_t n_Q \cdot \partial_t n_Q + B \partial_t n_S \cdot \partial_t n_S + C (n_Q \cdot \partial_t n_Q)^2 \right] \\ &\quad - f_{\parallel}^2 \left[ D_{\parallel} \nabla_a n_Q \cdot \nabla_a n_Q + E_{\parallel} \nabla_a n_S \cdot \nabla_a n_S + F_{\parallel} (n_Q \cdot \nabla_a n_Q)^2 \right] \\ &\quad - f_{\perp}^2 \left[ D_{\perp} \nabla_c n_Q \cdot \nabla_c n_Q + E_{\perp} \nabla_c n_S \cdot \nabla_c n_S + F_{\perp} (n_Q \cdot \nabla_c n_Q)^2 \right] + \dots, \end{aligned} \tag{21}$$

where  $f_t$ ,  $f_{\parallel}$  and  $f_{\perp}$  are constants, while  $V, A_{\parallel,\perp}, B_{\parallel,\perp}, C_{\parallel,\perp}, D_{\parallel,\perp}, E_{\parallel,\perp}$  and  $F_{\parallel,\perp}$  are potentially arbitrary functions of the  $SO(3) \times SO(2)$  invariants  $n_Q \cdot n_Q$  and  $n_S \cdot n_S$ . They also can depend on the temperature,  $T$ , since this can appear in  $\mathcal{L}$  through the process of integrating out the high-energy modes.

Fewer terms appear in eq. (21) than in eq. (5) because of the constraint  $n_S \cdot n_S + n_Q \cdot n_Q = 1$  which is enforced in (21), but not in (5). Should the ‘length’ of the  $SO(5)$ -breaking order parameter also describe a propagating mode in the low-energy system, as might be appropriate near the critical point, then this constraint may be relaxed. Since this mode is *not* guaranteed to be in the low-energy theory far away from the phase boundaries — unlike the pseudo-Goldstone states — we do not include it further in this section.

Far from the critical region the correlation length perpendicular to the planes becomes smaller than half the interplane spacing, and we take the system to be approximately two-

---

<sup>6</sup> Our notation here follows that of ref. [6], generalized to the anisotropic case. Other couplings, such as  $\epsilon^{mnl} \partial_m \vec{n}_S \cdot (\partial_n \vec{n}_S \times \partial_l \vec{n}_S)$ , are also possible in specific dimensions (in this case  $d=2$ ).

dimensional, corresponding to the limit <sup>7</sup>  $f_{\perp} = 0$ . We imagine working in this limit in what follows, and so from here on drop the redundant subscript ‘||’ from the coefficient functions  $D$ ,  $E$  and  $F$ .

Couplings to long-wavelength electromagnetic fields is incorporated in the effective theory through the usual substitution  $\partial_{\alpha}n_Q \rightarrow (\partial_{\alpha} - ieA_{\alpha}Q)n_Q$ . (A special case of this coupling is the dependence on the chemical potential,  $\mu$ , which enters  $\mathcal{L}$  through the replacement  $\partial_t n_Q \rightarrow (\partial_t - ie\mu Q)n_Q$  [17], [18].) For distances shorter than the electromagnetic screening length,  $a = eqf_t$ , this electromagnetic coupling includes the Coulomb interactions of the pseudo-Goldstone bosons. It is important to realize, however, that the strong *short-ranged* Coulomb interactions need not be included in this way, since these are integrated out to arrive at  $\mathcal{L}$  in the first place. Although strong microscopic interactions such as these would complicate the derivation of the  $\mathcal{L}$  from first principles, they play no role when using  $\mathcal{L}$  at low energies.

An important consequence of these observations now follows. When using the Lagrangian of eq. (21), the key observation is that all of the interactions are *guaranteed* to be weak at low energies, justifying a perturbative treatment. This is because all interaction terms are suppressed by either a derivative or a small  $SO(5)$ -breaking parameter or both. In particular, the pseudo-Goldstone spectrum may be obtained from  $\mathcal{L}$  in mean field theory by expanding in fluctuations about minima of the potential,  $V$ .

For later purposes a useful parameterization (which identically solves the constraint  $n_Q \cdot n_Q + n_S \cdot n_S = 1$ ) is given by polar coordinates on the four-sphere:

$$n_Q = \cos \theta \begin{pmatrix} \cos \phi \\ \sin \phi \end{pmatrix}, \quad n_S = \sin \theta \begin{pmatrix} \sin \alpha \cos \beta \\ \sin \alpha \sin \beta \\ \cos \alpha \end{pmatrix}, \quad (22)$$

(although care is required to properly handle those points where these coordinates are singular). In terms of these variables, and including a chemical potential, the Lagrangian

---

<sup>7</sup> A more detailed modelling of the dimensional crossover within the context of Bose-Einstein condensation is given in ref. [16].

becomes:

$$\begin{aligned}
\mathcal{L} = & -V + \frac{f_t^2}{2} \left[ \left( 1 + 2A \sin^2 \theta + 2B \cos^2 \theta + 2C \sin^2 \theta \cos^2 \theta \right) (\partial_t \theta)^2 \right. \\
& \left. + (1 + 2A) \cos^2 \theta (\partial_t \phi + eq\mu)^2 + (1 + 2B) \sin^2 \theta \left( (\partial_t \alpha)^2 + \sin^2 \alpha (\partial_t \beta)^2 \right) \right] \\
& - \frac{f_{\parallel}^2}{2} \left[ \left( 1 + 2D \sin^2 \theta + 2E \cos^2 \theta + 2F \sin^2 \theta \cos^2 \theta \right) (\nabla_a \theta)^2 \right. \\
& \left. + (1 + 2D) \cos^2 \theta (\nabla_a \phi)^2 + (1 + 2E) \sin^2 \theta \left( (\nabla_a \alpha)^2 + \sin^2 \alpha (\nabla_a \beta)^2 \right) \right] + \dots,
\end{aligned} \tag{23}$$

where all coefficient functions are to be regarded as functions of  $\cos^2 \theta$ .

To this point we have not yet used much information concerning the nature or size of the explicit symmetry breaking. This we now do by making an assumption as to how the symmetry-breaking terms transform under  $SO(5)$ . Since there are two types of symmetry breaking, a choice must be made for each.

- *Doping*: Doping has been incorporated into the effective theory through the chemical potential,  $\mu$ . We return to the connection between  $\mu$  and  $x$  in §3.3 below.
- *Intrinsic Breaking*: Symmetry breaking also occurs at half filling, with strength  $\epsilon$ . The resulting symmetry-breaking pattern is  $SO(5) \rightarrow SO(3) \times SO(2)$ . We assume this to be done with the simplest possible ‘order parameter’,  $M$ , which transforms in the adjoint representation of  $SO(5)$ . That is, choose  $M = \epsilon \text{diag}(3, 3, -2, -2, -2)$ .

The Lagrangian is then the most general function of the fields  $\mathbf{n} = \begin{pmatrix} n_Q \\ n_S \end{pmatrix}$ ,  $\mu Q$  and  $M$ , subject to the following  $SO(5)$  transformation property

$$\mathcal{L}(O\mathbf{n}, O\mu Q O^T, O M O^T) = \mathcal{L}(\mathbf{n}, \mu Q, M), \tag{24}$$

where  $O$  is an  $SO(5)$  transformation.

The utility of identifying  $Q$  and  $M$  may be seen when  $\mathcal{L}$  is expanded in powers of the small quantities  $\epsilon$  and  $\mu$ . Since  $M$  and  $Q$  always appear premultiplied by these small numbers, this expansion restricts the kinds of symmetry breaking which can arise order by order, which in turn constrains the possible  $\theta$ -dependence of the coefficient functions in  $\mathcal{L}$ .

For example, a term in the scalar potential involving  $2n$  powers of  $\mathbf{n}$  must have the following form:

$$V_{(n)} = \sum_{(k_1, l_1) \neq (0,0)} \cdots \sum_{(k_n, l_n) \neq (0,0)} C_{k_1 l_1, \dots, k_n, l_n} \left[ \mathbf{n}^T (\epsilon M)^{k_1} (\mu Q)^{2l_1} \mathbf{n} \right] \cdots \left[ \mathbf{n}^T (\epsilon M)^{k_n} (\mu Q)^{2l_n} \mathbf{n} \right]. \quad (25)$$

Only even powers of  $Q$  enter here due to its antisymmetry, and the term  $k_i = l_i = 0$  is excluded from the sums due to the constraint  $\mathbf{n}^T \mathbf{n} = 1$ . Expanding  $\mathcal{L}$  to low order in the  $SO(5)$ -breaking parameters  $\epsilon$  and  $\mu$  necessarily also implies keeping only the lowest powers of  $n_Q \cdot n_Q = \cos^2 \theta$  in  $V$ .

Similar conclusions may be obtained for the other coefficient functions in the Lagrangian of eq. (21). Working to  $O(\epsilon^2, \epsilon\mu^2, \mu^4)$  in  $V$ , and to  $O(\epsilon, \mu^2)$  in the two-derivative terms then gives:

$$V = V_0 + V_2 \cos^2 \theta + \frac{1}{2} V_4 \cos^4 \theta, \quad (26)$$

and

$$\begin{aligned} A &= A_0 + A_2 \cos^2 \theta, & B &= B_0 + A_2 \cos^2 \theta, & C &= C_0, \\ D &= D_0 + D_2 \cos^2 \theta, & E &= E_0 + D_2 \cos^2 \theta, & F &= F_0, \end{aligned} \quad (27)$$

for the coefficient functions in eq. (21). Notice that the terms proportional to  $\cos^2 \theta$  in  $A$  and  $B$  are identical, as are the corresponding terms in  $D$  and  $E$ . Expanding in powers of  $\epsilon$  and  $\mu$ , the constants in eqs. (26) and (27) start off linear in  $\epsilon$  and  $\mu^2$ :  $A_i = A_i^{10} \epsilon + A_i^{01} \mu^2 + \dots$  etc.. The only exceptions to this statement are:  $B_0, E_0 \propto \epsilon$  (no  $\mu^2$  term),  $C_0, F_0 \propto \mu^2$  (no  $\epsilon$  term), and  $V_4 = V_4^{20} \epsilon^2 + V_4^{11} \epsilon \mu^2 + V_4^{02} \mu^4$ . Furthermore, since the  $\mu^2 n_Q \cdot n_Q$  term in  $V$  arises from substituting  $\partial_t \rightarrow \partial_t - ie\mu Q$  in the kinetic term for  $n_Q$ , we have:  $V_2^{01} = -\frac{1}{2} f_t^2 e^2 q^2$  to leading order. Higher powers of  $\mu$  originate from terms in  $\mathcal{L}$  which involve more than two derivatives.

In this way we arrive at an effective lagrangian very similar to that of ref. [1] (in the isotropic limit). The main difference here is the power counting of the symmetry breaking terms. Ref. [1] keeps terms quadratic in  $n_Q$  and has three susceptibility parameters controlling the time-derivative terms, and three stiffness constants governing the spatial derivatives. Although a quadratic scalar potential captures the leading order in  $\epsilon$ , it does

not appear that a three-parameter derivative term corresponds to any fixed order in  $\epsilon$  or  $\mu^2$ .

### 3.2) Pseudo-Goldstone Dispersion Relations

We now turn to the calculation of the pseudo-Goldstone boson dispersion relations. The scalar potential of eq. (23) has three types of extrema:

- (1)  $\theta_0 = 0$  or  $\pi$ ;
- (2)  $\theta_0 = \frac{\pi}{2}$  or  $\frac{3\pi}{2}$ ;
- (3)  $\theta_0$  where  $c = \cos \theta_0$  satisfies  $V'(c^2) = 0$ .

This leads to the four classical ordered phases found in §2.2: (i) SC phase: extremum (1) is a minimum, and (2) is a maximum; (ii) AF phase: (2) is a minimum, and (1) is a maximum; (iii) MX phase: both (1) and (2) are maxima, and (3) is a minimum; or (iv) metastable phase: both (1) and (2) are minima, and (3) is a maximum. This analysis becomes identical to that of §2.2 if  $V$  is assumed to be quartic in  $\cos \theta$ , as was done in ref. [6].

- *Superconducting Phase:* An expansion about the superconducting minimum,  $\theta_0 = 0$ , gives the dispersion relations in this phase for the four bosons. The result is a spin triplet of pseudo-Goldstone modes for which

$$E(k) = \left[ c^2 k^2 + \mathcal{E}^2 \right]^{\frac{1}{2}}, \quad (28)$$

with the phase speed,  $c_{pGB}^2(SC)$ , and gap,  $\mathcal{E}_{pGB}^2(SC) \equiv \mathcal{E}_{SC}^2$ , given to lowest order in  $SO(5)$ -breaking parameters by:

$$\begin{aligned} c_{pGB}^2(SC) &= \frac{f_{\parallel}^2}{f_t^2} \left[ 1 + 2 \left( E(1) - B(1) \right) \right] \\ &= \frac{f_{\parallel}^2}{f_t^2} \left[ 1 + 2 \left( E_0 - B_0 \right) + 2 \left( D_2 - A_2 \right) \right], \\ \mathcal{E}_{SC}^2 &= \frac{-2V'(1)}{f_t^2} \\ &= \frac{-2(V_2 + V_4)}{f_t^2}. \end{aligned} \quad (29)$$

In both of these results the first equation uses the general effective theory, eq. (23), while the second equality incorporates the additional information of eqs. (26) and (27).

The remaining field,  $\phi$ , describes a *bona fide* gapless Goldstone mode. Its dispersion relation,  $E(k)$  is a more complicated function of  $c^2 k^2$  and  $eq\mu$  whose form [18], is not required here. Its phase velocity,  $c^2 \equiv c_{GB}^2(SC)$ , is given by

$$\begin{aligned} c_{GB}^2(SC) &= \frac{f_{\parallel}^2}{f_t^2} \left[ 1 + 2 \left( D(1) - A(1) \right) \right] \\ &= \frac{f_{\parallel}^2}{f_t^2} \left[ 1 + 2 \left( D_0 - A_0 \right) + 2 \left( D_2 - A_2 \right) \right]. \end{aligned} \quad (30)$$

Recall in these expressions that  $V(\cos^2 \theta)$  includes any  $\mu$ -dependent contributions coming from the kinetic terms, or their higher-derivative counterparts, and a prime denotes differentiation with respect to  $\cos^2 \theta$ .

• *Antiferromagnetic Phase:* Expanding about the AF minimum gives the usual two magnons satisfying dispersion relation (28), with:

$$\begin{aligned} c_{GB}^2(AF) &= \frac{f_{\parallel}^2}{f_t^2} \left[ 1 + 2 \left( E(0) - B(0) \right) \right] \\ &= \frac{f_{\parallel}^2}{f_t^2} \left[ 1 + 2 \left( E_0 - B_0 \right) \right], \\ \mathcal{E}_{GB}^2(AF) &= 0. \end{aligned} \quad (31)$$

The remaining two states form a pair of electrically-charged pseudo-Goldstone bosons satisfying:

$$E_{\pm}(k) = \left[ c^2 k^2 + \mathcal{E}^2 \right]^{\frac{1}{2}} \pm eq\mu, \quad (32)$$

with:

$$\begin{aligned} c_{pGB}^2(AF) &= \frac{f_{\parallel}^2}{f_t^2} \left[ 1 + 2 \left( D(0) - A(0) \right) \right] \\ &= \frac{f_{\parallel}^2}{f_t^2} \left[ 1 + 2 \left( D_0 - A_0 \right) \right], \\ \mathcal{E}_{AF}^2 = \mathcal{E}_{pGB}^2(AF) &= \frac{2V'(0)}{f_t^2} \\ &= \frac{2V_2}{f_t^2}. \end{aligned} \quad (33)$$

These expressions imply the simple formulae of ref. [6]:  $\mathcal{E}_{AF}^2 = m^2 - \kappa\mu^2$ , and  $\mathcal{E}_{SC}^2 = -m^2 + \kappa\mu^2 - \xi\mu^4$ , where  $m^2 \equiv 2V_2^{10}\epsilon/f_t^2 + O(\epsilon^2)$ ,  $\kappa \equiv -2V_2^{01}/f_t^2 + O(\epsilon) = e^2q^2 + O(\epsilon)$  and  $\xi \equiv 2V_4^{02}/f_t^2 + O(\epsilon)$ .

Within the AF phase the pseudo-Goldstone boson gap is seen to fall linearly with  $\mu^2$ :  $\mathcal{E}_{AF}^2 \approx \mathcal{E}_{AF}^2(0)[\mu_{AF}^2 - \mu^2]$ , where  $\mu_{AF}$  represents the doping for which one leaves the AF regime. Similarly  $\mathcal{E}_{SC}^2$  varies quadratically with  $\mu^2$ . By eliminating parameters of the Lagrangian in favour of properties of the gap as a function of  $\mu$  we find the relations of ref. [6]:

$$\begin{aligned}\mathcal{E}_{AF}^2(\mu) &= \frac{\mathcal{E}_{AF}^2(0)}{\mu_{AF}^2} [\mu_{AF}^2 - \mu^2], \\ \mathcal{E}_{SC}^2(\mu) &= \frac{\mathcal{E}_{SC}^2(\text{opt})}{\mu_{\text{opt}}^4} (\mu^2 - \mu_{SC-}^2)(2\mu_{\text{opt}}^2 - \mu^2), \\ \frac{\mathcal{E}_{AF}^2(0)}{\mu_{AF}^2} &= 2 \frac{\mathcal{E}_{SC}^2(\text{opt})}{\mu_{\text{opt}}^2}, \\ \mu_{AF}^2 &= \mu_{SC-}^2 + O(\epsilon^2),\end{aligned}\tag{34}$$

where  $\mu_{\text{opt}}$  here denotes the chemical potential corresponding to the maximum gap,  $\mathcal{E}_{SC}$ . We expect this to occur at optimal doping,  $\mu_{\text{opt}} = \mu(x_{\text{opt}})$ .

Similarly, the phase velocities for all modes in both SC and AF phases are equal to one another, and to  $f_t^2/f_{\parallel}^2$ , in the strict  $SO(5)$ -invariant limit. (The parameters  $f_t$  and  $f_{\parallel}$  are related to the compressibility and magnetic penetration depth in the next section.) The  $O(\epsilon)$  corrections to this limit also satisfy some model-independent relations, which follow by eliminating parameters from the above expressions:

$$c_{\phi}^2(SC) - c_{\phi}^2(AF) = c_{\alpha}^2(SC) - c_{\alpha}^2(AF) = O(\epsilon).\tag{35}$$

### 3.3) The Connection Between $x$ and $\mu$

The previous expressions giving the dependence of physical quantities in terms of the chemical potential,  $\mu$ , would be more useful if expressed in terms of the physically-measured quantity, the doping,  $x$ . This relation is determined implicitly in the present section.



The dependence  $\mu(x)$  is found by adjusting  $\mu$  to ensure that the net electric charge equals  $x$  charge carriers per unit cell. This must be done differently in the AF and SC phases.

In both phases the total charge is carried by both the charged pseudo-Goldstone states, *and* the ordinary electron-like quasiparticles responsible for conduction. The existence of these electron-like quasiparticles at low energies in the SC phase is demanded by the evidence in favour of a  $d_{x^2-y^2}$ -wave gap in the cuprate superconductors [19]. These experiments argue for the existence of ungapped states due to the nodes of the  $d_{x^2-y^2}$ -wave gap function, which cannot be provided by the four pseudo-Goldstone modes. In the AF phase these degrees of freedom correspond to ordinary unpaired electrons.

- *AF Phase:* In the AF phase the charge is carried by a mixture of electrons and charged pseudo-Goldstone states. The condition of equilibrium between these two types of charge carriers implies their electric chemical potentials must be equal, and so the defining condition for  $\mu(x)$  becomes:

$$\langle \rho_{\text{em}} \rangle \equiv \frac{ex}{\mathcal{V}} = \int_0^\infty d\omega \left\{ \mathcal{N}_F(\omega) [n_F(\mu) - n_F(-\mu)] + \mathcal{N}_B(\omega) [n_B(\mu) - n_B(-\mu)] \right\}, \quad (36)$$

where  $\mathcal{N}_F$  and  $\mathcal{N}_B$  respectively denote the density of states for fermions and bosons. For weakly interacting bosons in  $d$  spatial dimensions, whose dispersion relation is  $E^2 = k^2 c^2 + \mathcal{E}^2$ , the density of states is given explicitly by  $\mathcal{N}_B = (\Omega_d / (2\pi)^d) k^{d-2} E / c^2$ , where  $\Omega_d$  is the solid angle swept out by a vector in  $d$  spatial dimensions (so  $\Omega_2 = 2\pi$  and  $\Omega_3 = 4\pi$ ). The Bose-Einstein distributions are given by  $n_F(\mu) = [e^{(\omega - e\mu)/kT} + 1]^{-1}$  and  $n_B(\mu) = [e^{(\omega - qe\mu)/kT} - 1]^{-1}$ .

For small  $\mu$  it is the fermions which dominantly contribute to  $\rho$ , and the dependence  $x(\mu)$  which results is (for  $d = 2$  space dimensions) linear:  $x \propto \mu/J$ . This linear dependence changes once  $\mu$  becomes of order the scalar gap at zero doping,  $\mathcal{E}_{AF}(0) = O(\epsilon^{1/2}J)$ , since at this point the scalar charge density varies strongly with  $\mu$ , signalling the transition to the condensed (SC) phase.

§2.2 showed the doping for which one exits (at low temperature) from the AF phase to

be, in order of magnitude,  $x = x_{AF} = O(\epsilon^{1/2})$ . We see that this corresponds to a chemical potential whose size is  $\mu \equiv \mu_{AF} = O(\epsilon^{1/2}J)$ . (An identical conclusion regarding the size of  $\mu_{AF}$  may be drawn from the condition for Bose-Einstein condensation:  $\mu \simeq \mathcal{E}_{AF}(0)$ .)

We see that since the chemical potential depends linearly on doping within the AF regime, eqs. (34) implies a linear dependence of  $\mathcal{E}_{AF}^2(x)$  on  $x^2$ :

$$\mathcal{E}_{AF}^2(x) = \mathcal{E}_{AF}^2(0)(x_{AF}^2 - x^2). \quad (37)$$

Corrections to this linearity in  $x^2$  arise as the SC phase is approached since  $\mu$  no longer varies linearly with  $x$  near the point where the bosons condense.

• *SC Phase:* Deep within the SC phase we assume the charge density to be dominated by the  $n_Q$  condensate. Writing the potential as  $V(n) \approx \frac{1}{2}(m^2 - \nu^2)n^2 + \frac{1}{24}g^2n^4$  (where  $\nu \equiv eq\mu f_t$ ,  $m^2 \equiv 2V_2(\mu = 0) \approx 2V_2^{10}\epsilon$ , and  $g^2 = 12V_4(\mu = 0) \approx 12V_4^{20}\epsilon^2$ ), we see  $\langle \rho_{em} \rangle$  is given by

$$\langle \rho_{em} \rangle \equiv \frac{eqx}{\mathcal{V}} = - \left. \frac{\partial V}{\partial \mu} \right|_{n=n_0} = \frac{6eqf_t\nu}{g^2} (\nu^2 - m^2), \quad (38)$$

where  $n_0 = 6(\nu^2 - m^2)/g^2$  minimizes  $V$ . This leads to the asymptotic expressions  $\nu \approx (g^2x/6\mathcal{V}f_t)^{1/3} \propto x^{1/3}$  if  $g^2\langle \rho_{em} \rangle / (6f_tm^3) \gg 1$ , and  $\nu - m \approx gx/(12\mathcal{V}f_tm^2) \propto x$  if  $g^2\langle \rho_{em} \rangle / (6f_tm^3) \ll 1$ .

In the case of interest we have (for  $d = 2$  space dimensions)  $f_t = O(1)$ ,  $m^2 = O(\epsilon J^2)$ , and  $g^2 = O(\epsilon^2 J)$ , and so  $g^2\langle \rho_{em} \rangle / (6f_tm^3) \simeq x\epsilon^{1/2}/(6\mathcal{V}J^2)$ . Taking  $J \simeq 0.1$  eV and  $\mathcal{V} \simeq (10\text{\AA})^2$  we find  $6\mathcal{V}J^2 \simeq 10^{-5}$ , leading to  $g^2\langle \rho_{em} \rangle / (6f_tm^3) \simeq 10^5x\epsilon^{1/2} \simeq 10^4x$ . Since this is much greater than unity when  $x \gtrsim x_{SC} = O(\epsilon^{1/2})$ , it follows that  $\mu \propto x^{1/3}$  within the SC phase.

We may now determine the size of  $\mu$  at optimal doping. We found in §2.2 that optimal doping occurs for  $x = x_{opt} = O(1)$ , and so  $x_{opt}/x_{AF} = O(\epsilon^{-\frac{1}{2}})$ . But since  $\mu \propto x^{1/3}$  within the SC phase, we see  $\mu_{opt} \sim \mu_{AF}(x_{opt}/x_{AF})^{1/3} = O(\epsilon^{1/3})$ .

Together with the previous results, eqs. (34), these expressions imply that  $\mathcal{E}_{SC}^2(x)$  is quadratic in the variable  $\mu^2 \propto x^{2/3}$ . Similarly, the gap in the SC phase at optimal doping

is related to the AF gap at zero doping by:

$$\mathcal{E}_{SC}(\text{opt}) = \frac{\mu_{\text{opt}}}{\sqrt{2}\mu_{AF}} \varepsilon_{AF}(0) = O(\epsilon^{1/3} J). \quad (39)$$

This last equation, together with the interpretation of the 41 meV state as the pseudo-Goldstone boson of the SC phase, and the underlying electronic scale  $J \simeq 0.1$  meV, give the order of magnitude of the symmetry-breaking parameter:  $\epsilon \simeq 1\%$ .

#### 4. Response Functions

In order to measure the properties of these pseudo-Goldstone particles, it is necessary to understand how they contribute to the spin and electromagnetic response functions of the materials. This is the topic of the present section. Because these particles are weakly coupled, their response may be computed perturbatively.

As we shall see, it shall become important for these purposes also to understand how the pseudo-Goldstone states couple to the other degrees of freedom in the low-energy system. For this reason we also write down the electron/pseudo-Goldstone particle couplings in this section.

The starting point for calculating the response functions is to identify the dependence on the (pseudo-) Goldstone bosons of the spin and electromagnetic currents. These are very easily obtained, to lowest order in the derivative expansion, by constructing the corresponding Noether currents using the Lagrangian of eq. (21):

$$\begin{aligned} \rho_{\text{em}} &= -f_t^2 (1 + 2A) n_Q Q \partial_t n_Q, & \vec{\rho}_{\text{spin}} &= f_t^2 (1 + 2B) \vec{n}_S \times \partial_t \vec{n}_S, \\ \mathbf{j}_{\text{em}}^{\parallel} &= f_{\parallel}^2 (1 + 2D_{\parallel}) n_Q Q \nabla n_Q, & \vec{\mathbf{j}}_{\text{spin}}^{\parallel} &= -f_{\parallel}^2 (1 + 2E_{\parallel}) \vec{n}_S \times \nabla \vec{n}_S, \\ j_{\text{em}}^z &= f_{\perp}^2 (1 + 2D_{\perp}) n_Q Q \nabla_c n_Q, & \vec{j}_{\text{spin}}^z &= -f_{\perp}^2 (1 + 2E_{\perp}) \vec{n}_S \times \nabla_c \vec{n}_S. \end{aligned} \quad (40)$$

Because the pseudo-Goldstone bosons are weakly coupled, correlations of these currents may be directly evaluated for free bosons,  $n_Q$  and  $n_S$ , plus perturbative corrections.

This perturbative evaluation conveniently organizes the contributions to the response according to which states are responsible. The following sections give some examples of such calculations.

#### 4.1) High-Energy Contributions

Even though the effective lagrangian only contains as degrees of freedom the states which actually appear in the low-energy spectrum, it nonetheless carries the information as to how states at higher energies contribute to response functions. The contributions of higher-energy states are incorporated as they are integrated out to produce the effective lagrangian itself, and so their contribution to correlation functions may be read directly from the lagrangian.

More precisely, imagine coupling to a long-wavelength electromagnetic field,  $A_\mu$ , or to a fictitious field,  $s_\mu^a$ , coupling to spin, by making the substitution:  $\partial_\alpha n_Q \rightarrow (\partial_\alpha - ieQA_\alpha) n_Q$  or  $\partial_\alpha n_S \rightarrow (\partial_\alpha - iT_a s_\alpha^a) n_S$ , with  $T_a$  and  $Q$  the matrix generators of  $SO(3)$  and  $SO(2)$ , as defined in eq. (4). The high-energy contribution to the electromagnetic and spin response may then be obtained by differentiating the effective Lagrangian twice with respect to  $A_\mu$  or  $s_\mu^a$ . The resulting correlation is proportional to  $\delta^d(\mathbf{x} - \mathbf{x}') \delta(t - t')$ , as would be expected for a mode which fluctuates on a scale much shorter than that over which the response is computed.

Making this substitution for the electromagnetic response leads to the magnetic penetration depth along the planes,  $\lambda$ , and the electric screening length (or compressibility),  $a$ . These are given by:

$$\left(\frac{1}{\lambda^2}\right)_{\text{h.e.}} = 4\pi\mu_0 e^2 q^2 f_{\parallel}^2 (1 + 2D) n_Q \cdot n_Q, \quad \left(\frac{1}{a^2}\right)_{\text{h.e.}} = 4\pi e^2 q^2 f_t^2 (1 + 2A) n_Q \cdot n_Q, \quad (41)$$

where  $\mu_0$  is the magnetic permeability of the material. The result in the ground state is obtained by using the ground-state configurations:  $n_Q \cdot n_Q = 1$  (SC) or  $n_Q \cdot n_Q = 0$  (AF).

Similarly, the spin response obtained in this way gives the high-energy contribution

to the paramagnetic susceptibility:

$$\left(\chi_{ab}\right)_{\text{h.e.}} = \mu_s^2 f_t^2 (1 + 2B) n_s T_a T_b n_s, \quad (42)$$

where  $\mu_s$  is the magnetic moment of the pseudo-Goldstone bosons. These depend on temperature, only through the weak dependence of coefficients  $f_t$ ,  $f_{\parallel}$ ,  $A$ ,  $B$  and  $D$ .

#### 4.2) Goldstone Poles

The next simplest contributions to response functions to compute are the poles which occur in the correlation of the currents for spontaneously broken (approximate) symmetries, due to the contribution of the corresponding (pseudo-) Goldstone states. This includes the superconducting contribution to the electromagnetic response in the superconductor, and the magnon contribution to the spin response in the antiferromagnet, in addition to the pseudo-Goldstone boson couplings to the additional  $SO(5)$  generators which rotate the spin and charge degrees of freedom into one another. These are given in perturbation theory by the Feynman graph of Fig. (3), which describes the direct creation and destruction of the Goldstone boson from the ground state by the current of interest.

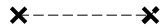


**Figure 3**

The Feynman diagram which produces the Goldstone pole contribution to the current-current correlation function. The dashed lines represent pGB propagation.

The result for the SC electromagnetic and the AF spin response, obtained by summing

the pole and the high-energy contributions, is:

$$\begin{aligned}
-i\theta(t) \langle [\rho_{\text{em}}(x, t), \rho_{\text{em}}(0)] \rangle_{GB} &= \int \frac{d^2k d\omega}{(2\pi)^2} e^{-i\omega t + ik \cdot x} \left[ \frac{4\pi e^2 q^2 (1 + 2A) f_t^2 k^2 c_{sc}^2}{-\omega^2 + k^2 c_{sc}^2 - i\gamma_{sc}\omega} \right], \\
-i\theta(t) \langle [\rho_{\text{spin}}^a(x, t), \rho_{\text{spin}}^b(0)] \rangle_{GB} &= \int \frac{d^2k d\omega}{(2\pi)^2} e^{-i\omega t + ik \cdot x} \left[ \frac{(1 + 2B) f_t^2 k^2 c_{af}^2 (n_s T_a \eta)(\eta T_b n_s)}{-\omega^2 + k^2 c_{af}^2 - i\gamma_{af}\omega} \right],
\end{aligned} \tag{43}$$

where  $c_{sc} \equiv c_{GB}(SC)$  and  $c_{af} \equiv c_{GB}(AF)$ .  $\gamma_{sc}$  and  $\gamma_{af}$  represents small damping contributions to the pGB dispersion relations. For the spin-spin correlation,  $\eta$  denotes the normalized eigenvector of the gap matrix corresponding to the GB direction whose pole is being computed. Notice eqs. (43) reproduce eqs. (41) and (42) in the limit  $\omega, k \rightarrow 0$ .

Of course, eqs. (43) are not specific to  $SO(5)$ -invariant physics, since they also hold for *any* antiferromagnet or superconductor. This is because they simply contain the implications of the Goldstone bosons associated with spontaneously broken  $SO(3)$  or  $SO(2)$  invariance. As a result, although they provide a good description of the response in these phases [20], [21], [7] this is not a real test of  $SO(5)$  symmetry.<sup>8</sup> It is the contributions of the *pseudo*-Goldstone states in both phases which provide more interesting information. After pausing to address a puzzle concerning the pseudo-Goldstone pole in the spin response of the SC phase, we close by describing some of the features of the pGB response.

#### 4.3) Pseudo-Goldstone Poles: A Puzzle

It was the contribution to neutron scattering of the spin-triplet pGB state in the SC phase which originally motivated the  $SO(5)$  picture. Since neutrons couple to electron spins, the  $SO(5)$  interpretation of the neutron-scattering experiments requires the pGB to contribute a resonance to the spin response functions.

This immediately leads to a puzzle. The spin-triplet pGB contributes a pole similar to eqs. (43) to three  $SO(5)$  currents (Zhang's  $\pi$  operators) which are spontaneously broken in the SC phase. But Fig. (3) does *not* produce a pole in the SC spin response function in the

---

<sup>8</sup> For the same reasons, neither are such responses detailed tests of the explicit models in which they are usually derived.

SC phase, because the symmetry of spin rotations is not broken in this phase. The puzzle is how such a pseudo-Goldstone pole can arise as a resonance in the SC spin correlation function. This section sketches how this puzzle is resolved within the effective field theory framework.

The difficulty with producing a pGB pole in the spin correlation function lies in the observation that  $\vec{\rho}_{\text{spin}}$  of eqs. (40) involves only *even* powers of the boson field,  $n_S$ . The same is true of the interactions in the effective lagrangian, eq. (21), and so it is difficult to generate a graph of the form of Fig. (4), which would generate a resonant contribution to the spin correlation function. The ‘blobs’ of Fig. (4) represent any graphs which can produce the triplet state starting from quasiparticles created by the spin density,  $\vec{\rho}_{\text{spin}}$ .

In our opinion the resolution of this puzzle comes from the couplings of the pseudo-Goldstone bosons to the electronlike quasiparticles in the SC phase. As stated earlier, the existence of these quasiparticles can be inferred from the evidence for  $d_{x^2-y^2}$ -wave pairing, since some of these experiments indicate the existence of gapless excitations in the SC phase. These excitations must be *in addition* to the four Goldstone and pGB states of the SC phase.

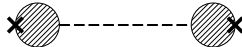


**Figure 4**

The Feynman diagram which produces the pole contribution to the spin correlation function in the SC phase due to the spin-triplet pseudo-Goldstone state. The ‘blobs’ represent fermion loops, while the dashed line represents pseudo-Goldstone boson propagation.

To see how these quasiparticles can help with the puzzle, suppose them to have the quantum numbers of electrons, and to have couplings that are weak, so that their propagation is approximately described by the Lagrangian density  $\mathcal{L}_0 = \int d^d p c_p^\dagger [i\partial_t - E_p] c_p$ . Here  $c_p = \begin{pmatrix} c_{p\uparrow} \\ c_{p\downarrow} \end{pmatrix}$  destroys a quasiparticle which propagates with dispersion  $\omega = E_p$ , as

is described by  $\mathcal{L}_0$ . Standard arguments [22], [23] can now be used to identify those interactions which are the most important in the long-wavelength limit. Goldstone boson couplings are all irrelevant (in the renormalization group sense) in this limit, but the least irrelevant of their couplings to the electronic quasiparticles involve the emission and absorption of a single Goldstone particle. The resulting electron Lagrangian density which describes this is:

$$\mathcal{L}_{\text{int}} = \int d^d p d^d k \left[ g_s(p, k) c_{p+k}^\dagger \vec{\sigma} c_p \cdot \vec{n}_Q(k) + g_Q(p, k) c_{p+k}^\dagger (i\sigma_2) c_{-p}^* n_Q(k) \right] + \text{h.c.} \quad (44)$$

This interaction is least irrelevant for special regions of momentum of the quasiparticle pairs [22], such as when the net momentum of the pair is close to zero.

Notice that an expectation value for  $n_Q$  introduces a quasiparticle gap, proportional to  $g_Q \langle n_Q \rangle$ , so a  $d_{x^2-y^2}$ -wave symmetry of the gap restricts how  $g_Q(p, k)$  can depend on momenta lying on the Fermi surface. Approximate  $SO(5)$  invariance relates the coupling  $g_Q(p, k)$  to  $g_s(p, k)$ , and so implies a similar  $d_{x^2-y^2}$ -wave symmetry for  $g_s(p, k)$ .

The principal observation at this juncture is that these quasiparticles contribute quadratically to the spin density,  $\vec{\rho}_{\text{elspin}} \propto \int d^d p c_p^\dagger \vec{\sigma} c_p$ , and so the coupling of eq. (44) introduces a pGB pole into the spin correlation function through the Feynman graph of Fig. (4), with the ‘blobs’ representing quasiparticle loops. Even though this graph does not arise at leading order in perturbation theory, the singular shape of the pole permits it to dominate the lower orders for energies and momenta which are related by the pGB dispersion relation.

#### 4.4) Pseudo-Goldstone Boson Response

Away from special features, such as the poles just discussed, the dominant contribution made by pseudo-Goldstone bosons to response functions arises through the Feynman graph of Fig. (5).



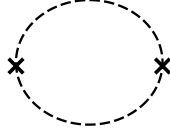


**Figure 5**

The Feynman diagram which produces the pseudo-Goldstone boson contribution to the electromagnetic response in the AF phase.

At zero frequency and momentum transfer this graph contributes a temperature- and doping-dependent contribution to the response functions, which are precisely those due to the noninteracting gas of bosons having the dispersion relation of the pseudo-Goldstone states. Since this dispersion relation is ‘relativistic’, the results are those of a gas of relativistic bosons [24].

In the SC phase one finds in this way the thermal paramagnetic susceptibility due to the spin-triplet pGBs:

$$\chi_{\text{pGB}}(SC) = \frac{2\mu_s^2 \Omega_d}{(2\pi c)^d} \int_0^\infty dx \frac{x^{d-3}}{E} \left[ x^2 + (d-2)E^2 \right] n_B(\mu = 0). \quad (45)$$

Recall  $\Omega_d$  is the solid angle swept out by a vector in  $d$  spatial dimensions ( $\Omega_2 = 2\pi$ ,  $\Omega_3 = 4\pi$ ), and the boson dispersion relation is  $E^2 = x^2 + \mathcal{E}^2$ , for  $x = kc$ . As in previous sections,  $n_B(\mu) = \left[ e^{\beta(E - eq\mu)} - 1 \right]^{-1}$  denotes the Bose-Einstein distribution function. The thermal electric screening length due to the charged pGBs of the AF phase is given by a very similar expression:

$$\left( \frac{1}{a} \right)_{\text{pGB}} (AF) = \frac{4\pi e^2 q^2 \Omega_d}{(2\pi c)^d} \int_0^\infty dx \frac{x^{d-3}}{E} \left[ x^2 + (d-2)E^2 \right] \left[ n_B(\mu) + n_B(-\mu) \right]. \quad (46)$$

Both  $\chi_{\text{pGB}}(SC)$  and  $(1/a)_{\text{pGB}}(AF)$  are therefore seen to be exponentially activated,  $\propto e^{-\beta\mathcal{E}}$ , for  $kT \ll \mathcal{E}$ , and to vary as  $T^{d-1}$  for  $kT \gg \mathcal{E}$ . Their contribution to the specific heat per unit volume,  $c_V$ , of the corresponding phases is also exponentially small for

$kT \ll \mathcal{E}$ , and varies as  $T^d$  for  $kT \gg \mathcal{E}$ . Unfortunately, the exponential suppression makes this  $T$  dependence difficult to detect at low temperatures, while the large- $T$  power-law behaviour only applies, as derived, for  $T$  much greater than the pGB gap, and yet small enough that the sample remains in the ordered phase.

The dynamic response function of a relativistic bose gas is also known for nonzero frequencies and momenta [25]. This carries considerably more information about the pseudo-Goldstone boson response, although the differentiation of the pGB contributions from other degrees of freedom is easiest at low frequencies. We close by presenting some preliminary remarks concerning this response, and defer a more detailed applications to experiments to a later publication.

Because of its electric charge, the pGB state of the AF phase cannot contribute to a diagram of the form of Fig. (4), and so give a pole at low temperatures in the electromagnetic response. Fig. (5) nevertheless does produce some strong dependence on frequency, due to the singularity it implies near the threshold for producing pairs of pGBs. Below this threshold the electromagnetic response from Fig. (5) is purely real, while it is complex above. As a result, for temperatures  $T \gtrsim \mathcal{E}_{AF}$  the pGBs contribute zero to the conductivity for frequencies below threshold,  $\omega \lesssim 2\mathcal{E}_{AF}$ , but the conductivity then grows steeply beyond this threshold. The implications of the resulting expressions for electromagnetic scattering from cuprates in the AF phase will be reported elsewhere.

#### 4.5) *The Disordered Phase*

Many of the results obtained above for pseudo-Goldstone bosons deep in the ordered phases might also be expected to apply in the disordered phase. If so, the wealth of experiments available there would permit many more detailed tests of  $SO(5)$  symmetry. Applications to the normal phase are also theoretically appealing, since a number of striking features might be expected within the  $SO(5)$  picture, including two of the more striking implications pointed out in ref. [1]: the explanation for the pseudogap, and of the connection to a successful scaling analysis of the temperature dependence of NMR relaxation times [26]. Furthermore, the absence of spontaneous breaking of  $SO(5)$  also

implies that the boson contribution to correlation functions of the  $SO(5)$  currents,  $j_a^\mu(x)$  – with  $a = 1, \dots, 10$  labelling the  $SO(5)$  generators – are very simply related in the  $SO(5)$ -invariant limit:  $\langle j_a^\mu j_b^\nu \rangle \propto \delta_{ab}$ .

In this section we make some *caveats* concerning the use of the effective lagrangians of previous sections in the disordered phase. Our main point is to emphasize that conclusions drawn from the effective lagrangian involving  $n_Q$ ,  $n_S$  (and possibly electronic quasiparticles) are *not* protected in the disordered phase by the general low-energy constraints of Goldstone’s theorem, and so are necessarily more dependent on assumptions made about the details of the underlying electronic interactions. Although this makes these predictions no longer simply consequences of the symmetry-breaking pattern, they can nevertheless be worthwhile as sources of more detailed information about this underlying microscopic physics.

We next describe some of the ways in which model dependence can enter predictions made for the disordered phase using the boson lagrangians described in this paper.

- *1. Degrees of Freedom:* First, the system’s real degrees of freedom need not be as assumed, since no general principles require the existence of low-energy bosonic states described by  $n_Q$  and  $n_S$  if no spontaneous symmetry breaking occurs. An exception might be in the immediate vicinity of the transition line into one of the ordered phases, since continuity at this line would require the gap for the pseudo-Goldstone states of the disordered phase to still be small in the ordered phase. The deeper one moves into the disordered phase, the less one would generically expect the boson gaps to remain small compared to the intrinsic scale,  $J$ .

Furthermore, since the four pseudo-Goldstone states should fill out a linear representation of the unbroken  $SO(5)$  of the disordered phase, fluctuations in the modulus of the five-dimensional vector,  $\mathbf{n}$ , should also appear in the low-energy spectrum. This argues that the effective lagrangian of interest is of the form considered here for the free energy, (eq. (5) supplemented by time-derivative terms) rather than as was used for the pseudo-Goldstone bosons of the ordered phases (eq. (21)). These differ through the relaxation of the constraint  $n_S \cdot n_S + n_Q \cdot n_Q = 1$ , due to the fluctuations in the magnitude of

$SO(5)$ -breaking order parameter,  $\mathbf{n}$ .

- *2. Weak Coupling:* Even if the boson degrees of freedom exist at low energy, they need not be weakly coupled since (unlike Goldstone bosons) they are not required to decouple at low energies. It is noteworthy, however, that for weakly-coupled systems the electron-boson interactions given in eq. (44) are the only couplings between the electrons and bosons which can be marginal or relevant (in the RG sense of refs. [22]). By contrast, there are a number of self-couplings among the bosons which can be relevant or marginal in the infrared. Of course, the existence of strong couplings among the low-energy degrees of freedom doesn't necessarily invalidate the use of the effective lagrangian, it could just complicate the extraction of its predictions.

- *3. Bose-Einstein Condensation:* Even if the previous assumptions should apply to a particular system, it is still true that a weakly-coupled version of electrons and bosons cannot provide a good description for the cuprates in the disordered phase for dopings larger than optimal. This is because if the bosons  $n_Q$  are supposed to appear at low energies, and if their couplings are weak, then the relation,  $\mu(x)$ , between chemical potential and doping should be reasonably well described, as in §3.3, by a gas of free bosons and electrons. But this description always implies Bose-Einstein condensation for sufficiently large dopings, since for large enough  $x$  the bosons always 'win' and, by condensing, dominate the expression for the electric charge density. This cannot describe the observed *decrease* of the critical superconducting temperature with increasing doping, above optimal doping.

Further work is necessary to better explore these implications for the normal phase, and to more clearly identify which predictions of the effective lagrangian for this phase are model-specific, and which are more robust consequences of the symmetry-breaking pattern.

### Acknowledgments

We would like to thank Charles Gale, Richard MacKenzie, Rashmi Ray for helpful discussions, as well as J. Irving Kapusta and Louis Taillefer for their guidance through the literature. We thank Shou-Cheng Zhang for sharing his ideas with us about high

$T_c$  superconductors. This research was partially funded by the N.S.E.R.C. of Canada, F.C.A.R du Québec and the Norwegian Research Council.

## 5. References

- [1] S.-C. Zhang, *SO(5) Quantum Nonlinear  $\sigma$  Model Theory of the High  $T_c$  Superconductivity*, Stanford preprint, cond-mat/9610140.
- [2] H.A. Mook et al., *Phys. Rev. Lett.* **70** (1993) 3490;  
J. Rossat-Mignod et al., *Physica (Amsterdam)* **235C**, 59 (1994);  
H.F. Fong et al., *Phys. Rev. Lett.* **75** (1995) 316.
- [3] S. Weinberg, *Phys. Rev. Lett.* **29** (1972) 1698.
- [4] E. Demler and S.C. Zhang, *Phys. Rev. Lett.* **75** (1995) 4126;  
S. Meixner, W. Hanke, E. Demler and S.C. Zhang, Stanford preprint, cond-mat/9701217.
- [5] S. Weinberg, *Physica* **96A** (1979) 327.
- [6] C.P. Burgess and C.A. Lütken, preprint McGill-96/45 (cond-mat/9611070).
- [7] For summaries of typical phase diagrams see, *e.g.*, J.W. Lynn, *High Temperature Superconductivity*, Springer-Verlag, 1990;  
G. Burns, *High Temperature Superconductivity, An Introduction*, Academic Press, 1992.
- [8] D. Arovas, A.J. Berlinsky, C. Kallen and S.C. Zhang, preprint cond-mat/9704048.
- [9] For a review of the critical behaviour of the high- $T_c$  systems, see Q. Li in *Physical Properties of High-Temperature Superconductors*, Volume V, edited by D.M. Ginsberg, World Scientific, 1996.
- [10] We thank G.R. Zemba, as well as M.A. Martin-Delgado and J.R. Pelaez for correspondence concerning this point.
- [11] M.E. Fisher and D.R. Nelson, *Phys. Rev. Lett.* **32** (1974) 1350;  
R.A. Pelcovits and D.R. Nelson, *Phys. Lett.* **57A** (1976) 23; *Phys. Rev.* **B16** (1977) 2191;  
D.S. Fisher, *Phys. Rev.* **B39** (1989) 11783;

- D.H. Friedan, *Ann. Phys. (NY)* **163** (1985) 318.
- [12] M.E. Fisher, M.N. Barber and D. Jasnow, *Phys. Rev.* **A8** (1973) 1111;  
 B.I. Halperin, T.C. Lubensky and S.-K. Ma, *Phys. Rev. Lett.* **32** (1974) 292;  
 D.S. Fisher, M.P.A. Fisher and D.A. Huse, *Phys. Rev.* **B43** (1991) 130.
- [13] See, *e.g.*, P.M. Chaikin and T.C. Lubensky, *Principles of Condensed Matter Physics*, Cambridge University Press, 1995.
- [14] The formalism for describing the dynamics of Goldstone and pseudoGoldstone modes was developed within the context of the strong interactions by:  
 S. Weinberg, *Phys. Rev. Lett.* **18** (1967) 188; *Phys. Rev.* **166** (1968) 1568; *op. cit.*;  
 S. Coleman, J. Wess and B. Zumino, *Phys. Rev.* **177** (1969) 2239; E.C. Callan, S. Coleman, J. Wess and B. Zumino, *Phys. Rev.* **177** (1969) 2247;  
 J. Gasser and H. Leutwyler, *Ann. Phys.* **158** (1984) 142; *Nucl. Phys.* **B250** (1985) 465.
- [15] Two relatively recent reviews of the Goldstone boson formalism, including applications to condensed matter physics, are given by:  
 H. Leutwyler, *Nonrelativistic Effective Lagrangians*, Bern preprint BUTP-93/25;  
 C.P. Burgess, *An Introduction to Effective Lagrangians and their Applications*, lecture notes for the Swiss Troisième Cycle, Lausanne, June 1995.
- [16] A. Hærdig and F. Ravndal, *Eur. J. Phys.* **14** (1993) 171.
- [17] Kothari and Singh, *Proc. Roy. Soc.* **A178** (1941) 135;  
 P.T. Landsberg and J. Dunning-Davies, *Phys. Rev.* **138** (1965) A1049;  
 J.I. Kapusta, *Phys. Rev.* **D24** (1981) 426;  
 H.E. Haber and H.A. Weldon, *Phys. Rev. Lett.* **46** (1981) 1497; *Phys. Rev.* **D25** (1981) 502.
- [18] J. Bernstein and S. Dodelson, *Phys. Rev. Lett.* **66** (1991) 683;  
 K.M. Benson, J. Bernstein and S. Dodelson, *Phys. Rev.* **D44** (1991) 2480.
- [19] For a review of the evidence for  $d_{x^2-y^2}$ -wave pairing in the high- $T_c$  systems, see J.F.

- Annett, N. Goldenfeld and A.J. Leggett, in *Physical Properties of High-Temperature Superconductors*, Volume V, edited by D.M. Ginsberg, World Scientific, 1996;  
D.J. Scalapino, *Phys. Rep.* **250** (1995) 329.
- [20] T. Timusk and D.B. Tanner, in *Physical Properties of High-Temperature Superconductors*, Volume I, edited by D.M. Ginsberg, World Scientific, 1989.
- [21] J.M. Tranquada, *et.al.*, *Phys. Rev.* **B40** (1989) 4503;  
S. Shamoto *et.al.*, *Phys. Rev.* **B48** (1993) 13817.
- [22] J. Polchinski, *Effective Field Theory of the Fermi Surface*, in *Recent Developments in Particle Theory, Proceedings of the 1992 TASI*, eds. J. Harvey and J. Polchinski (World Scientific, Singapore, 1993);  
R. Shankar, *Renormalization Group Approach to Interacting Fermions*, *Rev. Mod. Phys.* **66** (1994) 129;  
T. Chen, J. Fröhlich and M. Seifert, *Renormalization Group Methods: Landau-Fermi Liquid and BCS Superconductor*, preprint cond-mat/9508063.
- [23] C.P. Burgess, *op. cit.*
- [24] J.I. Kapusta, *Phys. Rev.* **D41** (1990) 6668; *Phys. Rev.* **D46** (1992) 4749;  
V.L. Eletsky, J.I. Kapusta and R. Venugopalan, *Phys. Rev.* **D48** (1993) 4398.
- [25] C. Gale and J.I. Kapusta, *Nucl. Phys.* **B357** (1991) 65;  
A.I. Titov, T.I. Gulamov and B. Kämpfer, *Phys. Rev.* **D53** (1996) 3770.
- [26] A. Sokol and D. Pines, *Phys. Rev. Lett.* **71** (1993) 2813.